RESEARCH ARTICLE
doi: 10.2306/scienceasia1513-1874.2018.44.011

ScienceAsia 44 (2018): **11–17**

Interfacial tension of turmeric nanoparticles

Sakchai Auychaipornlert[a], Pojawon Prayurnprohm Lawanprasert[a,*], Suchada Piriyaprasarth[b], Pongtip Sithisarn[c]

[a] Department of Manufacturing Pharmacy, Faculty of Pharmacy, Mahidol University, Bangkok 10400 Thailand
[b] Department of Pharmaceutical Technology, Faculty of Pharmacy, Silpakorn University, Nakhon Pathom 7300, Thailand
[c] Department of Pharmacognosy, Faculty of Pharmacy, Mahidol University, Bangkok 10400 Thailand

*Corresponding author, e-mail: pojawon.pra@mahidol.ac.th, pojawonpra@gmail.com

Received 12 Jun 2017
Accepted 23 Nov 2017

ABSTRACT: The dried rhizome of turmeric (*Curcuma longa*) is a source of volatile oil and curcuminoids. Curcumin, the major component, has a wide spectrum of pharmacological activities. Various advanced techniques have been proposed to improve the efficacy of curcumin, especially nanoparticles formation techniques. In this study, we prepared turmeric spherical particles in an alcoholic water system to investigate their physicochemical properties. Turmeric spherical particles were in a nanometre size range with a narrow size distribution and negative surface charge. Additionally, we proposed an equation derived from the Young-Laplace equation which appears to be applicable to estimate an interfacial tension value of turmeric nanoparticles and other microemulsion systems.

KEYWORDS: turmeric extract, modified Young-Laplace equation, microemulsion

INTRODUCTION

Turmeric, the dried rhizome of *Curcuma longa*, is a source of volatile oil and curcuminoids. Approximately 7% of yellow volatile oil contains turmerone and zingiberene as the major constituents and many other sesquiterpenes and monoterpenes. Curcuminoids is another group of component that occurs as yellow colouring matter which comprises curcumin (1.8–5%), desmethoxycurcumin, and bisdesmethoxycurcumin[1]. Although curcumin, a hydrophobic polyphenol, has a wide spectrum of pharmacological activities, its physicochemical properties, aqueous solubility, stability, and bioavailability are poor[2–5]. Thus there is a limitation for its use as a therapeutic agent. Various techniques were proposed to improve the efficacy of curcumin, for example, micelle[6–8], liposome[9], microemulsion[10–12], nanoemulsion[13,14], nanoparticles[15,16], nanocapsules[17–19], self-assembling peptide hydrogel[20], or solid lipid particle[21].

Microemulsion is a colloidal system of two immiscible liquids in which droplet formation requires low energy or occurs spontaneously[22]. Microemulsion is classified as thermodynamically stable whereas emulsion is classified as thermodynamically unstable. The difference of free energy before and after emulsification or free energy of formation (ΔG-formation), proposed by Hunter[23], who showed that the system can be spontaneously formed when the free energy of the system is negative; that is the interfacial tension should be very low. Interfacial tension plays an important role in microemulsion formation and stability[22,24]. There are several methods used for measuring surface tension or interfacial tension, for example, capillary rise, DuNoüy ring, drop weight, bubble pressure, pendent drop, and sessile drop. Unfortunately, these methods are not suitable for measuring the interfacial tension of microemulsion system because once an immiscible liquid contacts with another immiscible liquid, it is immediately dispersed and droplets are formed. In such case, interfacial tension may be determined by applying Young-Laplace equation

$$P_\alpha - P_\beta = 2\gamma/r, \tag{1}$$

where P_α and P_β are the internal and external pressures of the spherical droplet, respectively, γ is the surface tension or interfacial tension, and r is the radius of the spherical droplet[25].

We found that turmeric extract could form tiny spherical particles spontaneously when comes in contact with water. The objective of this study was to estimate the interfacial tension of spontaneous particle formation of turmeric extract in an alcoholic

water system by application of the equations used to describe the behaviour of a microemulsion system.

MATERIALS AND METHODS

Materials

Turmeric (*C. longa*, Zingiberaceae) rhizome powder was purchased from a local shop in Bangkok, Thailand. Plant sample was identified by Assistant Professor Dr Pongtip Sithisarn, Department of Pharmacognosy, Faculty of Pharmacy, Mahidol University, Bangkok, Thailand. Ultrafiltration deionized water was produced by Central Research Unit of Faculty of Pharmacy, Mahidol University (Bangkok, Thailand). Absolute ethanol was purchased from RCI Labscan Limited (Samutsakorn, Thailand).

Preparation of turmeric extract and turmeric nanoparticles

Turmeric extract (TE) was prepared from turmeric powder and ethanol. The extract containing curcumin as an internal marker at a concentration of 17.0 mg/ml, was filtered through 0.45 μm nylon filter. The filtrate was stored in glass bottle with screw cap protected from light and kept at 4 °C until use.

Turmeric nanoparticles were prepared by addition of 0.4 g TE into 100 g water using a glass dropper. The vial was swirled 100 times after each drop to ensure that a homogeneous mixture was obtained.

Refractive index and density determination

Refractive index values of TE and alcoholic water mixture were measured by using refractometer (Abbe Refractometer NAR-3T, Japan) at wavelength of 589 nm under controlled room temperature of 25 ± 2 °C. The specific gravity of alcoholic water mixture was determined by pycnometer method at 25 ± 2 °C according to AOAC official method 945.06 "Specific gravity (Apparent) of distilled liquors"[26]. The density was calculated by multiplying the specific gravity with standard density of water at 25 °C, 0.997 g/ml[27].

Particle morphology

Particle morphology of turmeric nanoparticles was observed under bright field and fluorescence using an inverted microscope (Olympus model IX81, Japan) and a transmission electron microscope (TEM). For TEM, the sample was deposited onto a Formvar-coated copper grid and left to dry at room temperature and subsequently observed under transmission electron microscope (Philips model Tecnai 20 Twin, USA).

Particle size distribution and zeta potential measurement

Particle size distribution was characterized by using a dynamic light scattering technique on a Zetasizer Nano ZS (Malvern, UK). Zeta potentials were characterized by the laser Doppler electrophoresis technique on a Zetasizer Nano ZS.

Effect of water phase dilution on turmeric nanoparticles

Turmeric nanoparticle sample containing of 0.4% w/w TE in water was prepared. Then, this sample was diluted with water to obtain a concentration series of 0.2, 0.1, 0.05, and 0.025% w/w. All samples were prepared in triplicate. The particle size distribution and zeta potential of all samples were determined immediately within 15 min after sample preparation.

Effect of ethanol on turmeric nanoparticles formation

To study the effect of ethanol on turmeric nanoparticles formation, TE was added into the mixture of various concentrations of ethanol in water. Ten grams of ethanol in-water mixture at concentrations of 10, 20, 30, 40, 50% w/w were prepared in glass vials. Then 0.01 g of TE was then added into these vials. The vials were swirled for 100 times. The particle size distribution and zeta potential of the samples were determined immediately within 15 min after sample preparation.

Data analysis

The data obtained were evaluated and expressed as mean ± SD of triplicates. One-way ANOVA was used to compare means ($\alpha = 0.05$). All analyses were performed using PASW Statistics for Windows, version 18.0 (SPSS Inc., USA).

RESULTS AND DISCUSSION

Refractive index and density determination

Refractive index, specific gravity, and density values of TE and alcoholic water system are shown in Table 1.

Particle morphology

Particle morphology of turmeric nanoparticles observed under bright field and fluorescence using

Table 1 Refractive index (RI), specific gravity (SG) and density values.

Sample	RI	SG	Density (g/ml)
Deionized water	1.335	–	–
10% w/w EtOH†	1.339	0.983	0.980
20% w/w EtOH	1.346	0.969	0.966
30% w/w EtOH	1.352	0.953	0.951
40% w/w EtOH	1.357	0.935	0.932
50% w/w EtOH	1.360	0.913	0.910
Alcoholic TE	1.380	–	–

† ethanol in water.

inverted microscope and transmission electron microscope are shown in Fig. 1. TE could form spherical particles of approximately 200 nm diameter when dropped in water and gently stirred. It appears that turmeric oil and curcuminoids, the main components in turmeric extracts, play an important role in nanoparticles formation. The mechanism of turmeric nanoparticles formation was the same as that described for a microemulsion system. Turmeric oil was an oil phase, curcuminoids was an emulsifier, and ethanol was a co-emulsifier.

Effect of water phase dilution on turmeric nanoparticles

Particle size distribution and zeta potential data of turmeric nanoparticles are shown in Table 2. For all samples, the particles formed had nanometre size range with negative surface charge. No significant change ($p > 0.05$) in size, derived count rate, or zeta potential was found throughout the time of measurement, i.e., 2000 s or 33.3 min (p-values between 0.34 and 0.96 for z-average, 0.08–1.00 for derived count rate, and 0.28–0.92 for zeta potential). These indicate the particles were stable over the measurement. Furthermore, these particles seem to have a uniform size according to the observation of low polydispersible index (PDI) (0.16–0.18).

Table 2 Particle size distribution and zeta potential of turmeric nanoparticles in water (mean ± SD, $n = 3$).

TE (%)	Z-ave. (nm)	Count rate ($\times 10^5$ kcps)	PDI	ζ potential (mV)
0.424	183 ± 2	7.37 ± 0.07	0.18 ± 0.01	−46.5 ± 1.3
0.212	181 ± 1	5.55 ± 0.16	0.17 ± 0.00	−44.2 ± 0.6
0.106	175 ± 2	2.96 ± 0.21	0.16 ± 0.00	−41.8 ± 0.8
0.053	167 ± 2	1.14 ± 0.09	0.16 ± 0.00	−42.1 ± 1.6
0.027	163 ± 3	0.45 ± 0.07	0.16 ± 0.00	−42.2 ± 0.9

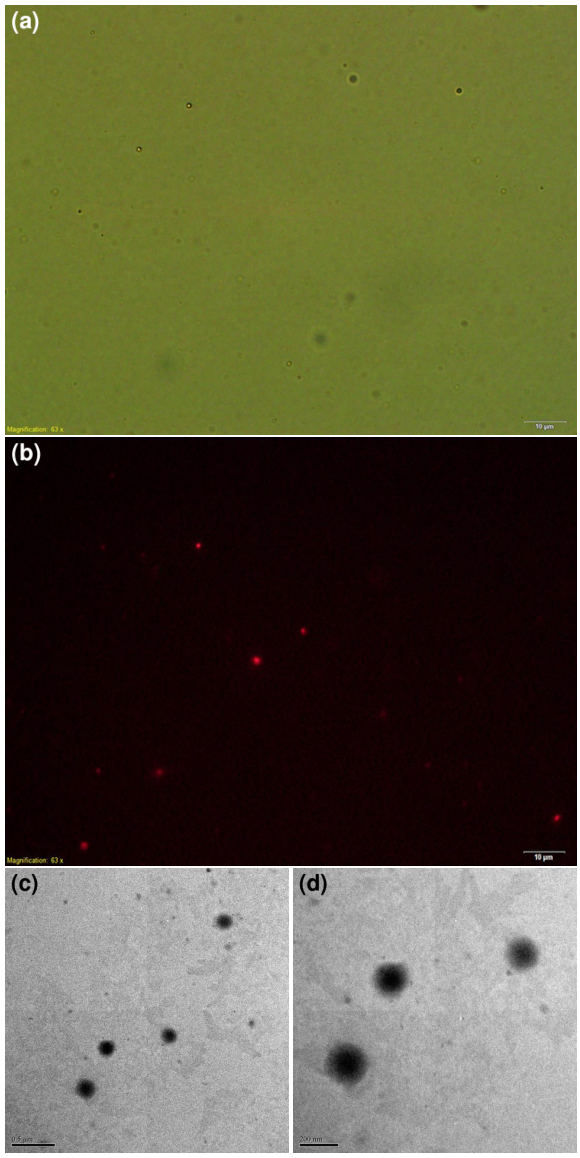

Fig. 1 Particle shape and physical appearance of the turmeric nanoparticles: (a) under bright field magnified 100×, (b) under fluorescence magnified 100×, (c) and (d) under TEM magnified 6500× and 14 500×, respectively.

From these results, it was shown that the particle size and the derived count rate decreased significantly when the sample was diluted ($p < 0.05$). The water dilution also resulted in significantly increased zeta potential values ($p < 0.05$). As the derived count rate is proportional to the concentration or number of particles in an aqueous phase and it can be used to estimate colloid concentrations[28,29], a decrease in derived count rate indicates that the

Table 3 Effect of ethanol concentrations on turmeric nanoparticles formation (mean ± SD, $n = 3$).

EtOH (w/w)	Z-ave. (nm)	Count rate ($\times 10^5$ kcps)	PDI	ζ potential (mV)
0%	183 ± 5	2.99 ± 0.14	0.20 ± 0.00	−48.3 ± 2.2
10%	231 ± 3	3.08 ± 0.19	0.15 ± 0.01	−32.2 ± 1.5
20%	285 ± 5	1.97 ± 0.08	0.10 ± 0.01	−22.0 ± 1.8
30%	313 ± 7	0.57 ± 0.05	0.08 ± 0.01	−14.5 ± 0.8
40%	356 ± 17	0.21 ± 0.05	0.08 ± 0.01	−10.7 ± 1.1
50%	315 ± 24	0.02 ± 0.01	0.22 ± 0.07	−5.4 ± 0.4

particle concentration decreased. In this case, the decrease in particle concentration resulted from the water dilution of the sample.

Effect of ethanol on turmeric nanoparticles formation

From the experiment, it was also found that, particles size, derived count rate, and zeta potential of turmeric nanoparticles did not change significantly throughout the measurement time (2000 s or 33.3 min) ($p > 0.05$). Furthermore, low PDI values were obtained, i.e., 0.08–0.22 (Table 3). This indicates that turmeric nanoparticles had uniform size in all alcoholic water systems. The results also show that ethanol quantity had an effect on particle size, size distribution, number of stable particles, and particle charge. It was found that, at ethanol concentration between 0 and 40% w/w, the higher ethanol concentration used, the larger turmeric particle size was obtained ($p < 0.05$). An increase in ethanol concentration from 40–50% w/w resulted in a decrease in particle size ($p < 0.05$). The smallest particle size of the system, 183 ± 5 nm, was obtained in water phase without ethanol.

Ethanol concentrations higher than 50% w/w were not employed in this study, as the results obtained in a preliminary study showed that turmeric nanoparticles could not be formed when ethanol concentration was higher than 50% w/w. This may be because all compositions of turmeric nanoparticles dissolved completely in that alcoholic system. This explanation could be supported by the results of derived count rate and zeta potential values. Derived count rate, which represents the number of particles in the system, tends to decrease significantly when ethanol concentrations was increased ($p < 0.05$). It was also found that zeta potential value of turmeric nanoparticles tends to increase when ethanol concentrations were increased ($p < 0.05$) (Fig. 2). Zeta potential demonstrated the surface charge of the nanoparticles. The minus value indicated that the surface charge of turmeric nanoparticles was negative. The increase in zeta potential value of turmeric nanoparticles may result from the loss of negative charge from turmeric nanoparticles surface. This phenomenon may be due to the increase in the solubility of certain compositions, which have negative charge, of turmeric nanoparticles into alcoholic water phase when ethanol concentration was increased.

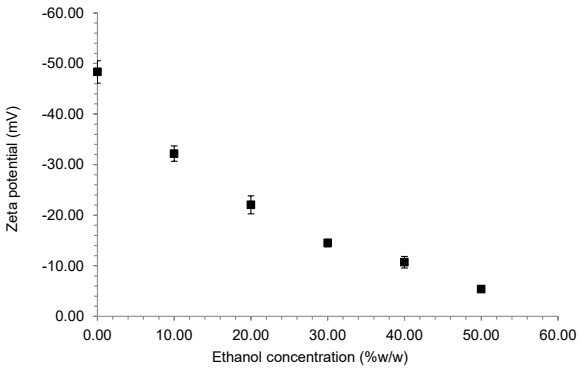

Fig. 2 Effect of ethanol concentrations on zeta potential of turmeric nanoparticles.

Theoretical considerations

An interfacial tension between the surface of turmeric nanoparticle and water phase after particle formation can be estimated by using the modified Young-Laplace equation below.

Consider an oil-in-water microemulsion system, oil droplets, usually spherical shape, are dispersed in the water phase. The pressure inside an oil droplet is always higher than the pressure outside the oil droplet according to Young-Laplace equation (1) [24,25,30]. In the case of an oil-in-water microemulsion system, the external pressure of the oil droplet is the sum of the hydrostatic pressure and the atmospheric pressure [30],

$$P_\beta = \rho g h + 1, \tag{2}$$

where ρ is the density of water phase, g is the gravitational acceleration, h is the depth of water phase, and the sea level standard atmospheric pressure is 1 atm. Substituting (2) into (1), we obtain

$$P_\alpha - \rho g h - 1 = 2\gamma / r. \tag{3}$$

For a pure water system,

$$P_{\alpha w} - \rho_w g h - 1 = 2\gamma_w / r_w, \tag{4}$$

where $P_{\alpha w}$, ρ_w, γ_w, and r_w are the internal pressure of oil droplet, the density of water phase, the interfacial tension, and the radius of oil droplet dispersed in pure water phase, respectively.

When the composition of the water phase is changed, the hydrostatic pressure is also changed due to the change in the density of water phase. This may have an effect on the internal pressure, interfacial tension, and the radius of oil droplet.

For an aqueous system

$$P_{\alpha m} - \rho_m g h - 1 = 2\gamma_m / r_m, \quad (5)$$

where $P_{\alpha m}$, ρ_m, γ_m, and r_m are the internal pressure of oil droplet, the density of water phase, the interfacial tension, and the radius of oil droplet dispersed in an aqueous system, respectively.

Subtracting (5) by (4) to obtain

$$(P_{\alpha m} - P_{\alpha w}) + (\rho_w - \rho_m) g h = \frac{2\gamma_m r_w - 2\gamma_w r_m}{r_m r_w}. \quad (6)$$

If the difference between interfacial tension of turmeric nanoparticles in pure water and aqueous system is negligible, that is $\gamma_w = \gamma_m = \gamma$, then (6) can be rearranged as

$$\frac{r_w - r_m}{r_m r_w} = \frac{gh}{2\gamma}(\rho_w - \rho_m) + \frac{P_{\alpha m} - P_{\alpha w}}{2\gamma}. \quad (7)$$

Eq. (7) expresses a linear relationship between the dependent variable, $y = (r_w - r_m)/r_m r_w$ and the independent variable, $x = \rho_w - \rho_m$. The line has a slope $gh/2\gamma$ and intercept $(P_{\alpha m} - P_{\alpha w})/2\gamma$. It is expected that this equation may be applicable to estimate an interfacial tension γ of turmeric nanoparticles and other microemulsion systems.

To estimate an interfacial tension γ of turmeric nanoparticles, $(r_w - r_m)/r_m r_w$ values were calculated (Table 4) and plotted against $\rho_w - \rho_m$ (Fig. 3).

From the graph, it can be seen that the relationship was not linear. This means that interfacial tension values between turmeric nanoparticles (dispersed phase) and aqueous systems containing different ethanol concentrations (continuous phase) varied depending on the concentration of ethanol. However, when restricting the ethanol concentration to 0–30% w/w, the plot was relatively linear ($r^2 = 0.9497$) (Fig. 4). In this case, the interfacial tension value could be calculated from the slope according to (7), where the gravitational acceleration g and the aqueous phase depth are 9.81 m/s^2 and 0.010 m, respectively. The calculated interfacial tension value of 9.87×10^{-4} mN/m was obtained. This value was considered to be low and the spontaneous formation of turmeric nanoparticles was possible. This explanation is consistent with the results obtained in this work and other research works.

As mentioned above, the spontaneous dispersion of one phase into another phase can only occur if the interfacial tension between the two phases is very low that the entropy can dominate the total free

Table 4 The calculated values according to modified Young-Laplace equation (7).

EtOH (w/w)	Density (kg/m^3)	$\rho_w - \rho_m$ (kg/m^3)	Particle size (nm)	$(r_w - r_m)/r_m r_w$ (10^6 m^{-1})
0%	997.0	0.0	183 ± 5	0.00
10%	980.3	16.7	231 ± 3	−1.12
20%	966.4	30.6	285 ± 5	−1.94
30%	950.6	46.4	313 ± 7	−2.26
40%	931.8	65.2	356 ± 17	−2.64
50%	910.2	86.8	315 ± 24	−2.28

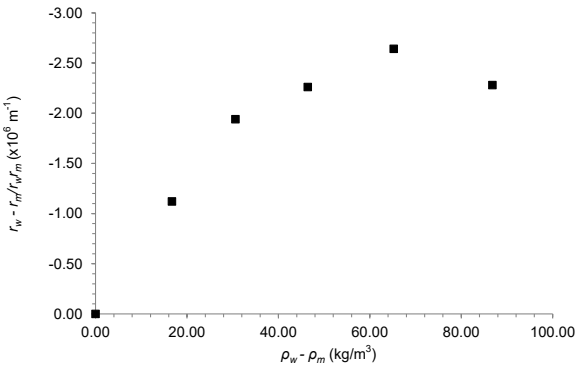

Fig. 3 Relationship between $(r_w - r_m)/r_m r_w$ and $\rho_w - \rho_m$ of turmeric nanoparticles.

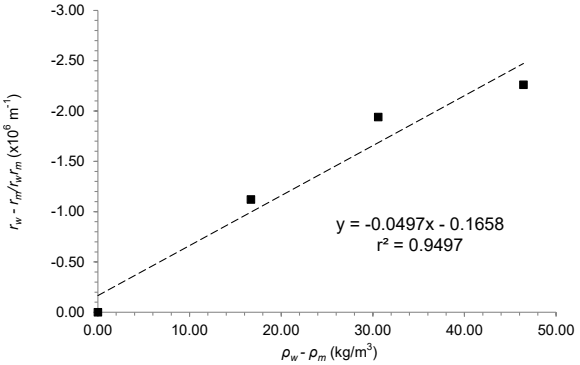

Fig. 4 Relationship between $(r_w - r_m)/r_m r_w$ and $\rho_w - \rho_m$ of turmeric nanoparticles for the ethanol concentration 0–30% w/w.

energy of the system[31]. Eastoe found that the interfacial tension produced by some surfactant is typically 10^{-2} to 10^{-4} mN/m [32]. Langevin stated that interfacial tension of a microemulsion system below 10^{-2} mN/m is low enough to compensate the dispersion entropy[33]. Langevin also found that common surfactants are unable to decrease interfacial tension below 1 mN/m. Cosurfactant such as short or medium chain alcohols was frequently added in order to lower the interfacial tension. Alcohol can reduce the rigidity of the interfacial film and promote more surfactant adsorption at the interface resulting in overall interfacial tension low enough for microemulsion formation[31]. Another explanation is that the relatively small size of alcohol molecule can be packed between surfactant molecules at the interface. The electrostatic and steric interaction between the surfactant head groups can be reduced resulting in densely packed of surfactant molecules at the interfacial layer, making the interfacial energy sufficiently low for a microemulsion to form spontaneously[31]. Consequently, relatively low interfacial tension, which leads to spontaneous turmeric nanoparticles formation in water phase as found in this work, may be due to the presence of naturally occurring negative charge surfactants in turmeric extract together with the effect of ethanol in the system. Furthermore, from the results, the size of turmeric nanoparticle was increased when ethanol concentration was increased up to 30% w/w. This phenomenon could be explained by the emulsion formation theory[34], which states that the diameter of the droplet formed ($a_{\max}$) depends directly on the interfacial tension (γ) and inversely on the energy density (ε) and the density of the continuous phase (ρ_c),

$$a_{\max} = C\varepsilon^{-2/5}\gamma^{3/5}\rho_c^{-1/5}. \quad (8)$$

In case of spontaneous turmeric nanoparticle formation obtained in this work, low or very low energy was required. Thus energy density was assumed to be low and may not significantly affect the size of turmeric nanoparticle. The interfacial tension value appears to be constant during ethanol concentration range of 0–30% w/w (Fig. 4). Hence in these cases, the diameter of turmeric nanoparticles depends mainly on the density of the continuous phase. From the results, the density of the alcoholic water system decreases as ethanol concentration increases. Hence the decrease of the density of alcoholic water systems results in an increase of the diameter of turmeric nanoparticles.

CONCLUSIONS

TE could form droplets or spherical particles in nanometre size range when dropped in water and gently stirred. These particles have negative surface charge. The particle size distribution was narrow and remained unchanged for a period up to 30 min. This may be due to very low interfacial tension of the system and to electrostatic repulsion between charged particles. It was found that ethanol quantity affected the particle size, size distribution, number of stable particles, and particle charge. The modified Young-Laplace equation proposed herein could be used to estimate interfacial tension values of the system. The results obtained in this work are consistent with the free energy of formation theory which states that spontaneous formation of an emulsion droplet will occur at low interfacial tension.

Acknowledgements: A special acknowledgement is extended to Faculty of Pharmacy, Mahidol University, Thailand for giving the best opportunity and providing research facilities. It is also extended to Silom Medical Co., Ltd., Thailand for supporting and providing fund.

REFERENCES

1. Jirawongse VA (1995) Khamin chan. In: *Thai Herbal Pharmacopoeia*, Prachachon, Bangkok, pp 38–44.
2. Anand P, Thomas SG, Kunnumakkara AB, Sundaram C, Harikumar KB, Sung B, Tharakan ST, Misra K, et al (2008) Biological activities of curcumin and its analogues (Congeners) made by man and Mother Nature. *Biochem Pharmacol* **76**, 1590–611.
3. Kunnumakkara AB, Anand P, Aggarwal BB (2008) Curcumin inhibits proliferation, invasion, angiogenesis and metastasis of different cancers through interaction with multiple cell signaling proteins. *Canc Lett* **269**, 199–225.
4. Sandur SK, Deorukhkar A, Pandey MK, Pabón AM, Shentu S, Guha S, Aggarwal BB, Krishnan S (2009) Curcumin modulates the radiosensitivity of colorectal cancer cells by suppressing constitutive and inducible NF-κB activity. *Int J Radiat Oncol Biol Phys* **75**, 534–42.
5. Srivastava RM, Singh S, Dubey SK, Misra K, Khar A (2011) Immunomodulatory and therapeutic activity of curcumin. *Int Immunopharmacol* **11**, 331–41.
6. Song L, Shen Y, Hou J, Lei L, Guo S, Qian C (2011) Polymeric micelles for parenteral delivery of curcumin: Preparation characterization and in vitro evaluation. *Colloid Surf A* **390**, 25–32.
7. Wan Z, Ke D, Hong J, Ran Q, Wang X, Chen Z, An X, Shen W (2012) Comparative study on the interactions of cationic Gemini and sigle-chain surfactant micelles with curcumins. *Colloid Surf A* **414**, 267–73.

8. Zhao L, Du J, Duan Y, Zang Y, Zhang H, Yang C, Cao F, Zhai G (2012) Curcumin loaded mixed micelles composed of Pluronic P123 and F68: Preparation, optimization and in vitro characterization. *Colloid Surf B* **97**, 101–8.
9. Karewicz A, Bielska D, Gzyl-Malcher B, Kepczynski M, Lach R, Nowakowska M (2011) Interaction of curcumin with lipid monolayers and liposomal bilayers. *Colloid Surf B* **88**, 231–9.
10. Ahmed K, Li Y, McClements DJ, Xiao H (2012) Nanoemulsion- and emulsion-base delivery systems for curcumin: Encapsulation and release properties. *Food Chem* **132**, 799–807.
11. Mohanty C, Sahoo SK (2010) The in vitro stability and in vivo pharmacokinetics of curcumin prepared as an aqueous nanoparticulate formulation. *Biomaterials* **31**, 6597–611.
12. Wang X, Jiang Y, Wang YW, Huang MT, Ho CT, Huang Q (2008) Enhancing anti-inflammation activity of curcumin through O/W nanoemulsions. *Food Chem* **108**, 419–24.
13. Cui J, Yu B, Zhao Y, Zhu W, Li H, Lou H, Zhai G (2009) Enhancement of oral absorption of curcumin by self-microemulsifying drug delivery systems. *Int J Pharm* **371**, 148–55.
14. Setthacheewakul S, Mahattanadul S, Phadoongsombut N, Pichayakorn W, Wiwattanapatapee R (2010) Development and evaluation of self-microemulsifying liquid and pellet formulations of curcumin, and absorption studies in rats. *Eur J Pharm Biopharm* **76**, 475–85.
15. Anitha A, Maya S, Deepa N, Chennazhi KP, Nair SV, Tamura H, Jayakumar R (2011) Efficient water soluble *O*-carboxymethyl chitosan nanocarrier for the delivery of curcumin to cancer cells. *Carbohydr Polymer* **83**, 452–61.
16. Konwarh R, Saikia JP, Karak N, Konwar BK (2010) 'Poly(ethylene glycol)-magnetic nanoparticles-curcumin' trio: Directed morphogenesis and synergistic free-radical scavenging. *Colloid Surf B* **81**, 578–86.
17. Lertsutthiwong P, Noomun K, Jongaroonngamsang N, Rojsitthisak P, Nimmannit U (2008) Preparation of alginate nanocapsules containing turmeric oil. *Carbohydr Polymer* **74**, 209–14.
18. Lertsutthiwong P, Rojsitthisak P, Nimmannit U (2009) Preparation of turmeric oil-loaded chitosan-alginate biopolymeric nanocapsules. *Mater Sci Eng C* **29**, 856–60.
19. Suwannateep N, Banlunara W, Wanichwecharungruang SP, Chiablaem K, Lirdprapamongkol K, Svasti J (2011) Mucoadhesive curcumin nanospheres: Biological activity, adhesion to stomach mucosa and release of curcumin into the circulation. *J Contr Release* **151**, 176–82.
20. Altunbas A, Lee SJ, Rajasekaran SA, Schneider JP, Pochan DJ (2011) Encapsulation of curcumin in self-assembling peptide hydrogels as injectable drug delivery vehicles. *Biomaterials* **32**, 5906–14.
21. Dadhaniya P, Patel C, Muchhara J, Bhadja N, Mathuria N, Vachhani K, Soni MG (2011) Safety assessment of a solid lipid curcumin particle preparation: Acute and subchronic toxicity studies. *Food Chem Toxicol* **49**, 1834–42.
22. Lawrence MJ, Rees GD (2000) Microemulsion-based media as novel drug delivery systems. *Adv Drug Deliv Rev* **45**, 89–121.
23. McClements DJ (2005) *Emulsion Stability in Food Emulsions: Principles, Practices, and Techniques*, 2nd edn, CRC Press, Florida.
24. Tadros T, Izquierdo P, Esquena J, Solans C (2004) Formation and stability of nano-emulsion. *Adv Colloid Interface Sci* **108–9**, 303–18.
25. Pellicer J, García-Morales V, Hernández MJ (2000) On the demonstration of the Young-Laplace equation in introductory physics courses. *Phys Educ* **35**, 126–9.
26. Latimer GW (2012) AOAC official method 945.06. In: *Official Methods of Analysis of AOAC International*, 19th edn, AOAC International, Maryland.
27. Lide DR (2010) *CRC Handbook of Chemistry and Physics*, 90th edn, CRC Press/Taylor and Francis, Florida.
28. Lahtinen M, Hölttä P, Riekkola ML, Yohannes G (2010) Analysis of colloids released from bentonite and crushed rock. *Phys Chem Earth* **35**, 265–70.
29. Wallace SJ, Li J, Nation RL, Boyd BJ (2012) Drug release from nanomedicines: selection of appropriate encapsulation and release methodology. *Drug Deliv Transl Res* **2**, 284–92.
30. Sinko PJ (2011) *Martin's Physical Pharmacy and Pharmaceutical Sciences*, 6th edn, Lippincott Williams & Wilkins, Philadelphia.
31. Ruckenstein E, Chi JC (1975) Stability of microemulsions. *J Chem Soc Faraday Trans II* **71**, 1690–707.
32. Eastoe J (2010) Microemulsion. In: Cosgrove T (ed) *Colloid Science: Principles, Methods and Applications*, 2nd edn, Wiley, West Sussex, pp 91–144.
33. Langevin D (1992) Micelles and microemulsions. *Annu Rev Phys Chem* **43**, 341–69.
34. Yang HJ, Cho WG, Park SN (2009) Stability of oil-in-water nanoemulsion prepared using the phase inversion composition method. *J Ind Eng Chem* **15**, 331–5.